IEEE Access
Multidisciplinary | Rapid Review | Open Access Journal

Received 24 June 2024, accepted 8 July 2024, date of publication 12 July 2024, date of current version 23 July 2024.

Digital Object Identifier 10.1109/ACCESS.2024.3427314

RESEARCH ARTICLE

Predictive Traffic Regulation Model for Railway Mass Transit Lines Equipped With Continuous Communication Systems

ÁLVARO CIDONCHA, ADRIÁN FERNÁNDEZ-RODRÍGUEZ, ASUNCIÓN P. CUCALA, AND ANTONIO FERNÁNDEZ-CARDADOR
Institute for Research in Technology, ICAI School of Engineering, Comillas Pontifical University, 28015 Madrid, Spain
Corresponding author: Antonio Fernández-Cardador (antonio.fernandez@iit.comillas.edu)

ABSTRACT Centralized traffic regulation systems are crucial in railway mass transit lines to automatically control the trains to recover delays and provide headway regularity. Traditional traffic regulation systems send control action to trains just at stations, through beacons, when they arrive or depart. The present paper proposes a new predictive traffic regulation model for railway mass transit lines equipped with CBTC (Communications Based Train Control) signalling system. This model takes advantage of continuous communications between the centralized control centre and trains, to send control actions at any moment. The proposed regulation system consists of two modules. The first one is a mathematical predictive control algorithm, which generates the running time and dwell time control actions by an optimization model based on the quantified delays of the trains and the operational constraints. The second module receives the control actions (target times) from the first one and generates in real-time the automatic driving commands to be sent to each train. This allows trains to modify their speed profile to speed up or slow down according to updated target times, at any point along their route. Finally, a traffic simulator based on a real Spanish metro line has been developed to verify the effectiveness of the proposed approach. Simulation results under normal operating conditions, considering random delays, show that adherence to the schedule and nominal headway improves by 33% and 49% respectively, and energy consumption is reduced by 5.4%.

INDEX TERMS ATO, ATR, CBTC, mass transit railway, railway traffic regulation.

I. INTRODUCTION

In recent decades, public subway transportation has become a key factor for sustainable urban development and the economic prosperity of cities. The use of this type of transportation entails a drastic reduction in greenhouse gas emissions, not only due to the use of electrical energy as the primary power source but also because it contributes to a decrease in the use of private vehicles.

Similarly, the exponential increase in urbanization has led to a significant rise in the demand for public transportation systems, causing congestion in these. The subway is considered a fundamental solution due to its high capacity, punctuality, and safety [1]. Moreover, the efficiency and reliability of the underground railway system are essential to ensure smooth and sustainable mobility in these cities. Consequently, the optimal management of railway traffic on subway lines has evolved into a complex challenge, prompting the search for new solutions to improve the quality of service provided to passengers, in terms of punctuality and headway regularity.

The implementation of Automatic Train Operation (ATO) in mass transit lines has contributed to improve the quality of service in metro lines achieving more regular and predictable travel times compared to manual operation, with better passenger comfort [2], and enables the automatic traffic control. This translates into a better experience, with an increased transport capacity and punctuality. Additionally, energy consumption is reduced because of the application of eco-driving techniques, which can be more accurately executed [3], [4], [5], [6].

The associate editor coordinating the review of this manuscript and approving it for publication was Emanuele Crisostomi.

Despite the benefits brought by ATO, the operation of high-frequency metro lines must deal with frequent disturbances. These disturbances cover from minor delays originated during the passengers unloading and loading at stations to major delays caused by door locks or other train failures. It is known that these lines are prone to instability because if a delay occurs in any of the trains, the accumulation of passengers at the station will lead to an increase in these delays [7]. Therefore, during traffic operation, corrections must be taken to prevent line instability.

Traditionally, the traffic corrections were performed by train drivers, who adapt the train speed and dwell time at stations to recover their own delays, and by the line traffic operators that dispatch trains in advance or hold trains departure based on the global traffic situation. On the other hand, in lines equipped with ATO systems, these corrections can be automatized.

Traffic corrections can be divided into two controlling levels. On one hand, a rescheduling level is needed when a big disturbance is detected and the goals of the planned timetable cannot be met. Numerous methods have been developed to detect and produce a new timetable that minimizes the disruption [8], [9], [10], [11], [12], [13]. Nowadays, in most metro lines, the rescheduling decisions are taken by line operators whose decisions can be supported by calculation methods like the previously mentioned.

On the other hand, traffic regulation level is needed constantly to prevent line instability, dealing with the frequent timetable deviations that do not impede the achievement of the planning goals. Automatic train regulation systems (ATR) have been developed and deployed along with ATO with this objective. ATR is a central control system that constantly supervises traffic performance and regulates the dwell time and the running time of trains [2]. The corrections produced by ATR could be oriented to adhere the train to the timetable or to maintain a balance between headway regularity and timetable punctuality. Nowadays, ATR systems are widespread in ATO metro lines where driving commands are automatically sent to the trains, as well as dwell time corrections.

ATR is based on a real-time traffic regulation algorithm. In the literature, various regulation algorithms have been proposed to enhance automatic traffic regulation. Among the early developments, heuristics algorithms were developed, standing out the one proposed by Araya and Sone [14]. In this algorithm, the control actions for train travel and stops are determined by a correction calculated based on the current deviation from the schedule and the deviation from the headway. A different heuristic approach is presented in [15], where an algorithm based on local optimality determines the most efficient strategies to correct the schedule when several trains travel close together. In reference [16] several heuristic algorithms are developed and compared. A predictive fuzzy controller was designed in [17] to control the dwell time at the station. The work presented in [18] proposes the use of genetic algorithms to recalculate the timetable when disturbances arise. A hybrid particle swarm optimization and genetic algorithm is proposed in [19] to adjust the timetable integrating the speed profile optimization modelled with a convolutional neural network. The passenger flow is modelled as a discrete Markovian process in [20], where a constrained state-space model is proposed. Some models have been proposed to directly minimize the passengers waiting time [21] by means of multi-objective optimization. The dwell time at stations and the coasting position of trains were obtained by a dual heuristic programming method for train regulation in [22]. Other approaches are based on automatic learning [23], which uses the characteristics of previous schedules to generate a new schedule with similar corrections as in the past. An adaptive optimal control approach based on reinforcement learning is proposed in [24] for train regulation.

The Model Predictive Control (MPC) [25] has become a widely used tool for traffic regulation to include real-time information about trains state and to meet the requirements of an online application [26]. It is crucial to deal with factors such as the long scale, nonlinearity, and stochastic events in transportation metro systems. Studies such as the one in reference [27] have compared models based on MPC strategy with heuristic regulators, demonstrating that the MPC strategy leads to better behavior. Pioneering approaches with this technology can be found in references [7] and [28], where the linear models proposed are very suitable for optimal state feedback without considering operational constraints. In [29], a classical optimization approach is presented to minimize the excess waiting time, travel time, and congestion after disturbances. In [30], a quadratic programming modelling is proposed to define an MPC strategy that includes the main operation constraints. The trade-off between passenger comfort and operating costs is considered in [31], and an Approximate Dynamic Programming method is used to solve the problem. A nonlinear optimal control model is presented in [32] to improve operational and energy efficiency considering the safety and control constraints. A distributed optimal control is proposed in [33] for complex metro networks. In [34], a heuristic method based on alternating directions of multipliers is proposed to compute the problem in a distributed manner. Several mixed-integer models have been presented to consider limitations on control actions and operational constraints such as a minimum headway between trains [35], to take into account the presence of disturbances in passenger arrival times [36], to consider stochastic disturbances due to uncertainties in train operation [37], to meet control requirements by transforming the optimization problem into a set of quadratic programming problems [38], to accelerate the process of schedule recovery [39], to minimize passenger travel costs [40] and to generate energy-efficient train regulation strategies considering peak power reduction [41] or energy storage [42]. The comfort of passengers has also been

included in optimization [43] by treating passenger behaviors as deterministic. Fuzzy logic is applied in [44] to include passenger flow uncertainty in robust traffic control. A robust fuzzy predictive control is proposed in [45] to account for the uncertainty of passenger arrival and imperfect wireless transmission.

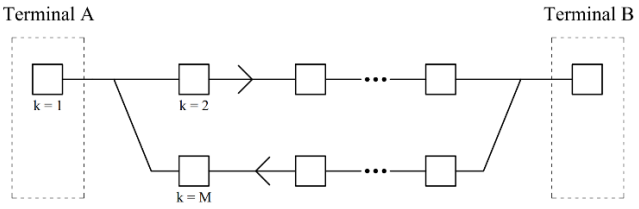

FIGURE 1. Loop line with terminal stations.

In previous models, the control actions resulting from optimization models and the detection of delays and incidents occur when trains depart or arrive at a station. However, modern signalling technologies, such as the Communication-Based Train Control (CBTC) technology [46], enable continuous communication between trains and the centralized system through a bidirectional radio communication system. That means that train position and delays supervision can be calculated continuously and, therefore, control actions can be executed when needed even if trains are travelling between stations. This communication capability of CBTC can be exploited to improve traffic regulation performance.

In this paper, it is proposed a predictive traffic regulation algorithm for a railway mass transit line equipped with CBTC technology, which allows the calculation and execution of control actions at any point along the route without having to wait for trains to arrive at stations. The contributions of this algorithm include a continuous delay supervision method to evaluate the current adherence of trains to timetable and headway objectives. Based on that information, the main contribution of this approach is the generation of updated ATO driving commands when control actions provided by the algorithm are recalculated for trains running between stations, permitting the early correction of delays.

The main operational constraints, such as minimum intervals between trains associated with the signalling system, the capacity of train delay recovery at each interstation, and dwell times limits, are included in the model.

Additionally, a simulator of a mass transit line has been developed to test the behavior of the algorithm in comparison to traditional regulation systems, proving that the proposed approach leverages the advantages of the CBTC technology to enhance the traffic operation of the line, and additionally to improve the associated energy consumption.

Section II introduces the regulation problem and the structure of the proposed traffic regulation model. Then, in Section III, the traffic regulation model for CBTC is described which is composed of two modules: the mathematical predictive control algorithm and the ATO driving commands generator. Section IV describes the simulator of the real mass transit line used to test the proposed algorithm. Sections V and VI present the results and the conclusions, respectively.

II. PROBLEM DESCRIPTION

It is considered a mass transit loop line where terminal stations are modeled as turnback platforms as presented in Fig. 1. Trains travel in both directions along a closed circuit, stopping along their journey at stations with one platform in each direction. Traffic is modeled as a set of N trains ($i = 1$ to N) circulating along M platforms ($k = 1$ to M), where each train i follows train $i - 1$ and stops at stations for passengers to get on and off.

The target of a centralized traffic regulation system is to recover the schedule when delays arise, balancing the importance of timetable punctuality and headway regularity. The traffic regulation system supervises the traffic measuring trains delays and calculates the control actions to be sent to each train in the line.

Nowadays, the traffic regulation systems are based on the centralized calculation of control actions and their dispatch at the stations arrivals and departures, which are the moments at which train delays are calculated. In this type of line equipped with discrete control center to train communication systems, only the sending of control actions to the train is allowed at those points, through beacons placed at the beginning and end of the station.

In addition, the bandwidth of the beacons is limited, so the information that can be transmitted is low. For this reason, a small number of different train driving commands can be sent to the train.

This paper proposes a new centralized predictive traffic regulation model for a railway mass transit line equipped with CBTC (Communication-Based Train Control) technology, where the control center can continuously quantify delays in the convoy trains and send run and stop control actions and ATO driving commands through a radio communication system at any moment. In addition, the associated high bandwidth permits the sending of numerous different driving commands to the train.

The interaction between the traffic regulation model and the simulator is schematically represented in Fig. 2.

The proposed model for automatic traffic regulation consists of two modules. The first one, the mathematical predictive control algorithm generates control actions by an optimization model based on the quantified delays of the trains and the operational constraints. These control actions calculated by this algorithm are the required increase or decrease of running time and stop time with respect to the nominal values for each train of the line. The second module calculates ATO driving commands to be sent to each train according to control actions provided by the predictive control algorithm.

Additionally, a simulator based on a real metro line has been developed to verify the effectiveness of the proposed

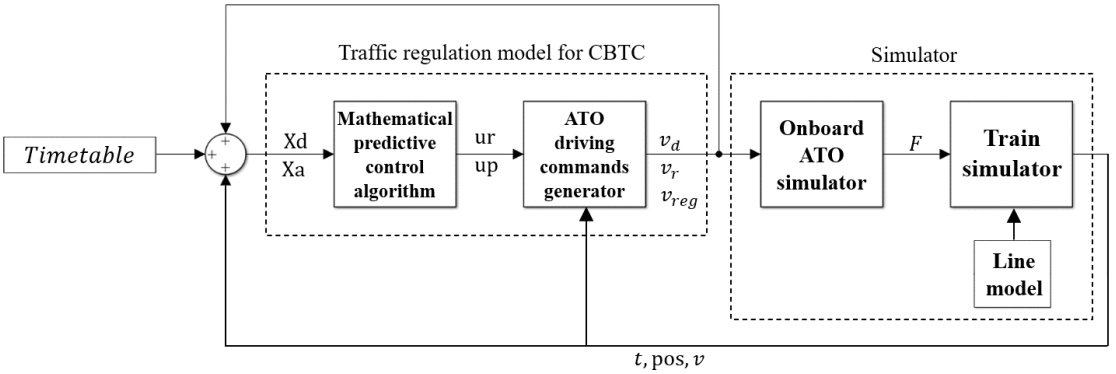

FIGURE 2. Algorithm and simulator structure.

approach. This simulator consists of a realistic ATO model, which receives the driving commands resulting from the traffic regulator model for CBTC and processes them to calculate the force that the train's motor must exert. Then, the multi-train simulator is executed with a dynamic model of each train of the metro line (Fig. 2) to calculate the train speed and position along the route taking into account how the signalling system affects the train motion. The essential variables in the model are described in Table 1.

In the following sections, the traffic regulation model for CBTC lines and the simulator are described.

III. TRAFFIC REGULATION MODEL FOR CBTC

In this section, the two modules of the proposed algorithm, which constitute the centralized control for automatic traffic regulation, will be detailed.

A. MATHEMATICAL PREDICTIVE CONTROL ALGORITHM

The mathematical predictive control algorithm (Fig. 2), calculates the running time and stop control actions based on the quantification of train delays using a quadratic programming optimization model. This model takes advantage of the continuous communication capabilities of CTBC systems, to control trains continuously according to traffic state.

The objective of the model is to minimize timetable and headway deviations of trains along a prediction horizon defined as the next L stations for each train. The control actions of the model are time corrections on the nominal running time and dwell time for each train and each station along the prediction horizon.

1) SCHEDULE DESIGNING

As it was mentioned before, traffic is modeled as a set of N trains ($i = 1$ to N) circulating along M platforms ($k = 1$ to M), where each train i follows train $i-1$ and stops at stations for passenger to get on and off.

Given a scheduled departure time Td_k^i for train i from platform k and a nominal stop time S_{0k} at platform k, the scheduled arrival time Ta_k^i of train i at platform k can be obtained as follows:

$$Ta_k^i = Td_k^i - S_{0k} \tag{1}$$

Under nominal operating conditions, there exists a nominal interval H between consecutive trains, where train i follows train $i-1$

$$H = Td_k^i - Td_k^{i-1} \tag{2}$$

With the nominal travel time R_k between platform k and platform $k+1$, the arrival time of train i at platform $k+1$ is obtained, if $k \leq M-1$:

$$Ta_{k+1}^i = Td_k^i + R_k \tag{3}$$

On the other hand, if $k = M$, it is necessary to establish a relation between the arrival at platform $k = 1$ and the departure of the platform M:

$$Ta_1^i = Td_M^i + R_M \tag{4}$$

2) TIMETABLE AND HEADWAY DEVIATION DEFINITION

At the departure time of the train from the platform and at the arrival time, the measured times are denoted as td_k^i and ta_k^i respectively. The associated measured headway of train i at departure of platform k (h_k^i) is defined as:

$$h_k^i = td_k^i - td_k^{i-1} \tag{5}$$

Thus, the following deviations can be defined:

- The deviation from the scheduled departure time Xd_k^i of train i at platform k

$$Xd_k^i = td_k^i - Td_k^i \tag{6}$$

- The deviation from the scheduled arrival time Xa_k^i of train i at platform k

$$Xa_k^i = ta_k^i - Ta_k^i \tag{7}$$

- Deviation from the nominal interval Y_k^i for train i measured at platform k departure. This deviation from nominal interval arises from the difference between the

TABLE 1. Variables description.

NOTATION	DESCRIPTION
α_k	Proportional constant involved in the extra stop time at platform k due to delays.
a	Weighting factor of run-time control action.
b	Weighting factor of stop-time control action.
c	Weighting factor of the slack variable.
H	Nominal headway between consecutive trains.
h_k^i	Measured headway of train i at departure from platform k.
I_{mink}	Minimum interval at platform k arrival.
L	Number of platforms in the optimization horizon.
M	Number of platforms.
N	Number of trains.
p	Weighting factor of timetable deviation.
pos	Actual train position.
q	Weighting factor of headway deviation.
R_k	Nominal travel time between platform k and platform $k+1$.
S_{0k}	Nominal stop time at platform k.
s_k^i	Stop time of train i at platform k.
sg_k^i	Positive slack variable that allows long running times for the train i from platform k to $k+1$.
t	Actual train time.
Ta_k^i	Nominal arrival time of train i at platform k.
ta_k^i	Actual arrival time of train i at platform k.
Td_k^i	Nominal departure time of train i at platform k.
td_k^i	Actual departure time of train i at platform k.
to_k	Objective running time from platform k to platform $k+1$.
up_k^i	Control action that modifies the nominal dwell time of train i at platform k.
UPmin_k	Control action that adds the minimum comfortable time to the dwell time at station k.
UPmax_k	Control action that adds the maximum comfortable time to the dwell time between at station k.
ur_k^i	Control action that modifies the nominal run time of train i from platform k to platform $k+1$.
URmin_k	Control action that adds the minimum comfortable time to the running time between the station k and $k+1$.
URmax_k	Control action that adds the maximum comfortable time to the running time between the station k and $k+1$.
v	Actual train velocity.
v_d	Coasting velocity.
v_r	Remotoring velocity.
v_{reg}	Speed regulation command.
X^i	Current delay of train i.
Xa_k^i	Deviation from de scheduled arrival time of train i at platform k.
Xd_k^i	Deviation from de scheduled departure time of train i at platform k.
Y_k^i	Deviation from the nominal headway for train i measured at platform k departure.

headway of a train i at platform k and the nominal headway:

$$Y_k^i = h_k^i - H \tag{8}$$

The previous equation can be expressed as:

$$\begin{aligned} Y_k^i &= (\mathrm{td}_k^i - \mathrm{td}_k^{i-1}) - (\mathrm{Td}_k^i - \mathrm{Td}_k^{i-1}) \\ &= (td_k^i - Td_k^i) - (td_k^{i-1} - Td_k^{i-1}) \end{aligned} \tag{9}$$

Consequently, it is easy to deduce:

$$Y_k^i = Xd_k^i - Xd_k^{i-1} \tag{10}$$

3) TRAFFIC MODEL

The traffic regulator corrects the timetable and headway deviations modifying the trains' nominal run time between two consecutive platforms and the nominal stop time at platforms. The optimization model includes the main operational constraints defined by the following traffic equations.

The signalling system is included in the traffic control model considering the minimum headway constraint. In metro-type lines the arrival time of a train i to a platform k is restricted by the departure time from k of the preceding train $i-1$:

$$ta_k^i - td_k^{i-1} \geq I_{mink} \tag{11}$$

where I_{mink} is the minimum interval at platform k arrival. Subtracting the nominal time equations (1) and (2) from (11), the following time deviation is obtained.

$$\mathrm{Xa}_k^i - \mathrm{Xd}_k^{i-1} \geq I_{mink} + S_{0k} - H_n \tag{12}$$

The running time of train i from platform k to $k+1$ verifies:

$$\mathrm{ta}_{k+1}^i - \mathrm{td}_k^i = R_k + \mathrm{ur}_k^i + \mathrm{sg}_k^i \tag{13}$$

where ur_k^i is the train i control action that modifies its nominal run time from platform k to $k+1$, and sg_k^i is a positive slack variable that allows long running times (greater than comfortable running times) when trains have to brake due to signalling intervention to maintain the minimum interval.

The control actions are bounded, that is:

$$\mathrm{URmin}_k \leq \mathrm{ur}_k^i \leq \mathrm{URmax}_k \tag{14}$$

where URmax_k represents the control action that adds the maximum comfortable time to the running time between station k and $k+1$, and URmin_k represents the control action that subtracts the most time from the run time between station k and $k+1$ (defined by flat-out driving).

Subtracting equation (3) from the previous run time constraint equation (13), a time deviation expression is obtained

$$\mathrm{Xa}_{k+1}^i - \mathrm{Xd}_k^i = \mathrm{ur}_k^i + \mathrm{sg}_k^i \tag{15}$$

It is worth noting that, as the predictive traffic algorithm is equipped with CBTC technology, it is possible to recalculate the ATO's driving commands (up_k^i and ur_k^i) at any moment during the travel. Therefore, the optimization problem may be initiated while a train is traveling between stations. The model includes this situation considering, for the first station of the simulation horizon k_{0i}, the current delay of these trains, X^i, rather than their delay at the station departure Xd_k^i.

It is worth noting that if the train is stopped at a station, k_{0i} would be the index of that platform and if the train is travelling between two stations, k_{0i} would be the index of the platform where it has departed from. Therefore, the simulation horizon for train i starts in platform k_{0i} and ends in platform $k_{0i}+L$.

The calculation of current delays is detailed in Section IV.D. Consequently, equation (15) will be replaced by equation (16) for $k = k_{0i}$ if train i is traveling between stations.

$$\mathrm{Xa}^i_{k_{0i}+1} - X^i = \mathrm{ur}^i_{k_{0i}} + \mathrm{sg}^i_k \tag{16}$$

Additionally, for these trains is necessary to update the control actions limits $\mathrm{URmax}_{k_{0i}}$ and $\mathrm{URmin}_{k_{0i}}$. This is because the capability to recover and lose time is reduced during the train travel respect to the initial situation at the departure from the previous station. To obtain the new control actions limits, it will be necessary:

1. To obtain the lower limit $\mathrm{URmin}_{k_{0i}}$, a simulation from the train's current space-speed point running as close as possible to the maximum speed values is performed. This way, the minimum running time to the next station under this simulation scenario is measured. The lower limit $\mathrm{URmin}_{k_{0i}}$ is obtained by subtracting this minimum running time from the nominal one.
2. To obtain the upper limit $\mathrm{URmax}_{k_{0i}}$, a simulation from the train's current space-speed point running at a minimum comfortable speed is performed. This way, the maximum running time to the next station under this simulation scenario is measured. The upper limit $\mathrm{URmax}_{k_{0i}}$ is obtained by subtracting this maximum running time from the nominal one.

As a clarification, Fig. 3 shows a graph where, after the start of a run of any interstation, the velocity of that interstation is presented from a current time T against time. In this representation, it has been assumed that the train follows a faster speed profile than the nominal speed profile. Besides, as mentioned before, it is necessary to simulate the fastest, slowest, and nominal speed profile from the current spatial point where the train is for the recalculation of the control limits to be valid.

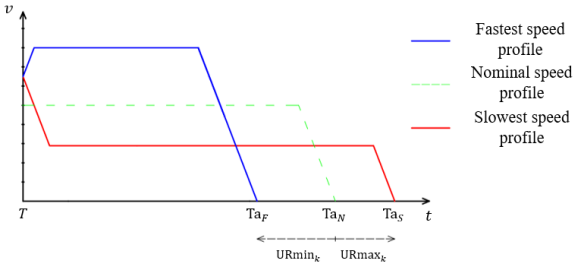

FIGURE 3. Schematical representation of the run control action limits.

So, when the current time of the train is T according to Fig. 3, the arrival time at the next station according to the nominal speed profile is Ta_N. Similarly, the shortest interstation run time from that current time T is obtained if the train adopts the fastest speed profile which is marked by the solid blue line, arriving at the station at time Ta_F. On the other hand, the longest interstation run time from that current time T is obtained if the train adopts the slowest speed profile which is marked, arriving at the next station at time Ta_S.

Consequently, equation (14) will be replaced in the traffic model by equation (17) if $k = k_{0i}$.

$$\mathrm{URmin}_{k_{0i}} \leq \mathrm{ur}^i_{k_{0i}} \leq \mathrm{URmax}_{k_{0i}} \tag{17}$$

On the other hand, the stop time at platforms is considered linear with respect to de departure-arrival interval given that the time required by passengers to get on and off increases with that interval. This assumption has been considered in references [7], [30], and [35] too. Consequently, the stop time s^i_k of train i at platform k is a function of the measured departure-arrival interval, the stop time control action up^i_k and a proportional constant α_k:

$$s^i_k = S_{0k} + \alpha_k \left(\mathrm{ta}^i_k - \mathrm{td}^{i-1}_k\right) + \mathrm{up}^i_k \tag{18}$$

The control action up^i_k is positive when the train i is held at platform k and negative when the stop time is reduced. Additionally, it is bounded between its maximum and minimum values, in a similar way as the ur^i_k control action:

$$\mathrm{UPmin}_k \leq \mathrm{up}^i_k \leq \mathrm{UPmax}_k \tag{19}$$

Also, it can be seen that $\mathrm{td}^i_k = \mathrm{ta}^i_k + s^i_k$. Subtracting it from equation (1):

$$\begin{aligned}&\mathrm{td}^i_k - \mathrm{Td}^i_k \\ &= \left(\mathrm{ta}^i_k + s^i_k\right) - \left(\mathrm{Ta}^i_k + S_{0k}\right) \\ &= \mathrm{ta}^i_k - \mathrm{Ta}^i_k + \alpha_k \left[\left(\mathrm{ta}^i_k - \mathrm{Ta}^i_k\right) - \left(\mathrm{td}^{i-1}_k - \mathrm{Td}^{i-1}_k\right)\right] + \mathrm{up}^i_k\end{aligned} \tag{20}$$

The time deviation expression is finally obtained:

$$\mathrm{Xd}^i_k - \mathrm{Xa}^i_k = \mathrm{Xs}^i_k + \mathrm{up}^i_k \tag{21}$$

where $\mathrm{Xs}^i_k = \alpha \left(\mathrm{Xa}^i_k - \mathrm{Xd}^{i-1}_k\right)$ is the delay in the stop due to passengers' accumulation.

When a train i is stopped when the optimization is initiated, the limits for the control actions UPmin_k and UPmax_k must be updated at the first station k_{0i} of the optimization horizon. Fig. 4 shows a representative diagram of the evolution of the time indicating the moment of the arrival Ta^i_k of train i at platform k, the moment where nominal stop time $\mathrm{Ta}^i_k + s_{0k}$ is met, the initial maximum limit UPmax_k and the initial minimum limit UPmin_k of the stop control action, as well as the four scenarios in which the train can be found during the stop.

In the first scenario, current time is less than the minimum departure time $\mathrm{Ta}^i_k + S_{0k} + \mathrm{Xs}^i_k - \mathrm{UPmin}_k$ (for instance when the current time is T_1 in Fig. 4). In this case, there is still capacity to recover or lose all the available time according to the limits of the stop control action, therefore UPmax_k and UPmin_k are the configured initial values.

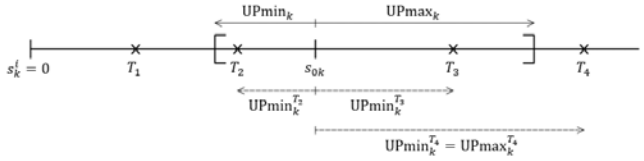

FIGURE 4. Schematic representations of the stop control action limits.

When the stop time has exceeded the value of the minimum departure time (scenarios 2 and 3), there is a loss of the capacity to recover time during the stop, so the lower limit of the stop control action UPmin_k must be updated. In both cases, this limit will be equal to the difference between the current time and $\text{Ta}_k^i + S_{0k} + \text{Xs}_k^i$. In the second scenario, when the current time is T_2 (lower than the departure applying the nominal dwell time), the limit of control action is negative, giving the train the possibility to recover delays in this stop. However, in scenario 3, when the current time is T_3 (greater than the departure applying the nominal dwell time), it will be positive losing the possibility to recover delays in this stop, resulting in an additional delay. The upper limit of the stop control action does not change in both cases, maintaining the configured initial value of UPmax_k.

Finally, in the fourth scenario, for instance when current time is T_4, current time is greater than the maximum departure time $\text{Ta}_k^i + S_{0k} + \text{Xs}_k^i + \text{UPmax}_k$. In this case, both the upper and the lower limits are equal to the difference between the current time and $\text{Ta}_k^i + S_{0k} + \text{Xs}_k^i$. Therefore, the only possible command is an immediate departure from the platform. It is worth noting that a stop control command, as defined in equation (18), is an increase or decrease time over the nominal dwell time (taking into account extra time due to passenger affluence). Therefore, an immediate departure order means that the stop control action will be equal to the difference between the current time spent at the station by the train and the nominal dwell time.

Equations (22) and (23) model previous update of lower and upper dwell limits for $k = k_{0i}$ if train i is stopped at a station, where T is the current time:

$$\text{UPmin}_{k_{0i}} = \max\left[\text{UPmin}_k, T - \left(\text{Ta}_k^i + S_{0k} + \text{Xs}_k^i\right)\right] \tag{22}$$

$$\text{UPmax}_{k_{0i}} = max[\text{UPmax}_k, T - (\text{Ta}_k^i + S_{0k} + \text{Xs}_k^i)] \tag{23}$$

Consequently, equation (19) will be replaced by equation (24) if $k = k_{0i}$.

$$\text{UPmin}_{k_{0i}} \leq \text{up}_{k_{0i}}^i \leq \text{UPmax}_{k_{0i}} \tag{24}$$

4) PREDICTIVE TRAFFIC CONTROL MODEL

A prediction horizon is defined, which contains the next L stations for which the arrival and departure delays are to be calculated for each train (Xa_k^i and Xd_k^i), as well as the travel and stop commands for each station (ur_k^i and up_k^i) and the slack variables sg_k^i.

The cost function that minimizes regularity criteria during the prediction horizon and the magnitude of control actions and slack variables is defined as:

$$J = p\sum_{i,k}\left(\text{Xd}_k^i\right)^2 + q\sum_{i,k}\left(\text{Xd}_k^i - \text{Xd}_k^{i-1}\right)^2 + a\sum_{i,k}\left(\text{ur}_k^i\right)^2 + b\sum_{i,k}\left(\text{up}_k^i\right)^2 + c\sum_{i,k}\left(\text{sg}_k^i\right)^2 \tag{25}$$

For each train $i : 1 \leq i \leq N$ and for each station $k : k_{0i} \leq k \leq k_{0i} + L$, where k_{0i} is the next departure station of train i and L is the number of stations included in the optimization horizon. Additionally, constants p and q represent the weight of the deviation from the nominal schedule and the deviation from the nominal interval, respectively. Similarly, constants a and b represent the weight of the control actions for run time and stop time, respectively. Finally, constant c represents the weight of the slack variable, large enough to minimize the intervention of signalling systems.

The initial conditions of the optimization problem are the position in the line and the delay of each train. For each train, there are two cases:

1. The train is stopped at station: It is necessary to stablish the deviation from the scheduled arrival time $\text{Xa}_{k_0}^i$ of train i at the first station k_0:

$$\text{Xa}_{k_0}^i = \text{Xa}_k^i \tag{26}$$

2. The train is traveling between stations: It is necessary to establish its current delay relative to the nominal schedule X_i at the current position of train i:

$$X^i = \text{Xd}_{k_0}^i + \Delta X \tag{27}$$

where $\text{Xd}_{k_0}^i$ is the departure delay of train i from the last station k_0, and ΔX is the running time difference between the real train driving and the nominal one from the departure of the last station up to the current train position. Positive values of ΔX represent delay increase from the last departure, and negative values represent delay recovery.

In CBTC lines (with continuous communication) it is possible to calculate delays X_i at any current position of the train. This permits the traffic regulation system to update control commands as soon as delays arise to better correct the incidences. In lines equipped with signalling systems based on discrete communications, these delays are updated (and corrected) just at the stations.

Finally, the optimization control problem is defined by its cost function described in equation (25); the initial conditions defined in equation (26) or (27) depending on each train initial state; the traffic model constraints for $k > k_{0i}$ outlined in equations (14), (15), (19) and (21); and the traffic model constraints for $k = k_{0i}$ outlined in equations (16), (17) or (21), (22), (23), (24) depending on each train initial state.

Commercial solvers for quadratic optimization problems can be used to solve this optimization. In this case, the lsqlin

solver integrated in MATLAB has been used, as detailed in Section V-C.

This optimization model is executed at regular time intervals (control cycle) to obtain the next dwell time control action up_k^i and the next running time control action ur_k^i.

B. ATO DRIVING COMMANDS GENERATOR FOR CBTC TECHNOLOGY

This subsection refers to the second module (Fig. 2) of the proposed traffic regulation model for CBTC, which transforms the control actions calculated by the Mathematical predictive traffic control algorithm (increase/decrease dwell time at stations or increase/decrease running times with respect to nominal values) into driving commands to be sent to each train.

The proposed Traffic regulation model for CBTC is based on continuous communication enabling continuous regulation as trains can receive control actions at any point along the journey. This represents an improvement in operational efficiency improving the response to disturbances.

The proposed traffic regulation system modifies the driving commands of the ATO in real time, at any moment. The type of driving commands of the ATO depends on the specific characteristics of the equipment (which depends on the manufacturer). The proposed traffic regulation model is based on one of type of ATO in service nowadays in many different metro lines. Specifically, the modelled ATO permits 2 types of driving: maintaining a constant speed defined by the speed regulation command v_{reg}, or driving with coasting-remotoring cycles based on the commands coasting velocity v_d and remotoring velocity v_r.

An interstation governed by a coasting velocity and a remotoring velocity is shown in Fig. 5. When the train is in traction and reaches the coasting velocity, the motor stops exerting force, and the train starts to coast, moving by its own inertia conditioned by the slope of the track. In case the train reaches the remotoring velocity, traction will be applied again until braking orders are given or another coasting point is reached (coasting speed). In any case, the train will brake to observe speed limitations and stopping points.

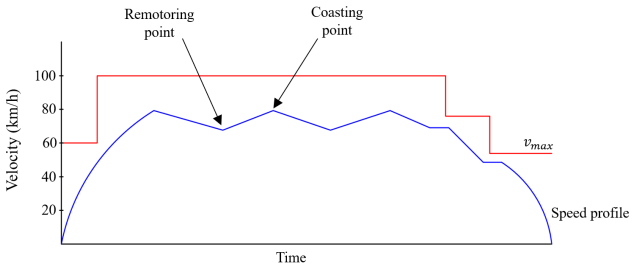

FIGURE 5. Interstation speed profile.

To update the ATO's driving commands in real-time, the model is executed at small time intervals to efficiently quantify delays. This strategy allows for more effective traffic regulation, resulting in shorter waiting times for passengers.

1) GENERATION OF DRIVING COMMANDS AT DEPARTURE

In existing traffic regulation systems, the set of driving commands that the controller can select and send to the trains is a reduced number, typically 4, due to limited communications. This set of driving speed profiles, from station departure to arrival at the next station, are usually pre-designed imposing restrictions on travel time, consumption, and passenger comfort. When the traffic regulation system calculates the time correction required for a train, it selects, from among the pre-designed commands, the one that is closest to the required time.

In the proposed model, thanks to the large bandwidth available, the set of pre-designed speed profiles for each inter-station can be much larger: a Pareto curve in which for each travel time the profile that minimizes consumption while meeting comfort requirements is designed [48]. In this way, traffic control can be more precise in the execution of the optimal travel time and will have a positive impact on both the quality of service and energy consumption.

When a train departs from station, the required running time to next station is calculated:

$$to_{k_{0i}} = R_{k_{0i}} + ur^i_{k_{0i}} \tag{28}$$

where $to_{k_{0i}}$ is the objective running time from initial station k_{0i} to estation $k_{0i}+1$ for train i, $R_{k_{0i}}$ is the nominal running time defined in the timetable for this stretch and $ur^i_{k_{0i}}$ is the correction time for the running time for this train calculated by the mathematical predictive control algorithm in the last execution.

The driving commands v_d, v_r or v_{reg} for this train are selected from the pre-designed Pareto front for the required objective running time $to_{k_{0i}}$.

2) UPDATE OF DRIVING COMMANDS ALONG THE INTERSTATION

On the other hand, in the proposed model based on continuous communication, the mathematical predictive control algorithm updates the control actions every control cycle when the train is on the route. Then, the ATO driving commands generator adapts the driving commands calculated at the departure as described in the following.

Consider a stretch between two stations k_{0i} and $k_{0i}+1$, where the movement of train i is governed by a coasting – remotoring type of driving. As can be seen in Fig. 6, the inputs of the proposed driving commands generator are the train's position pos, the train's time t, where $t=0$ at the moment the train departs from station k, the coasting velocity v_d, the remotoring velocity v_r, and the target running time $to_{k_{0i}}$. The objective of this module is to modify these ATO driving commands $v_d{}'$ and $v_r{}'$ to achieve this updated target time, even if it changes during the interstation.

The target time $to_{k_{0i}}$ from the current position of the train pos, to the next station is calculated as:

$$to_{k_{0i}} = R^{pos}_{k_{0i}} + ur^i_{k_{0i}} \tag{29}$$

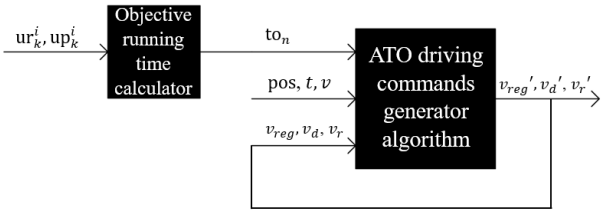

FIGURE 6. ATO driving commands generator algorithm.

where $R_{k_{0i}}^{\text{pos}}$ is the nominal running time from the current position of the train pos, to the next station and $ur_{k_{0i}}^i$ is the correction time for the running time for this train calculated by the mathematical predictive control algorithm in the last execution.

If all trains in the convoy adhere to the nominal schedule at the time of predictive optimization execution, the run control action $ur_{k_{0i}}^i$ will be null. Consequently, the target time $to_{k_{0i}}$ will coincide with the nominal time $R_{k_{0i}}^{pi}$, resulting in no changes in the ATO's driving commands (nominal driving).

Once the target running time $to_{k_{0i}}$ is calculated, the running time from the current train location up to the next station is simulated in a loop (using the simulation algorithm described in Section IV). In each iteration of this loop, the current coasting velocity v_d and remotoring velocity v_r are modified by a velocity increment Δv, small enough to achieve accurate resolution. This process continues until the simulated running time applying the modified commands is $to_{k_{0i}}$.

For the modification of these driving commands, two cases can be considered:

1. If the train is in traction mode (it is approaching the coasting point), the coasting velocity v_d and remotoring velocity v_r will be modified with the same speed increment Δv.
   However, it can be possible that, due to the restriction (30) that the remotoring velocity cannot be lower than a minimum remotoring velocity vr_{min}, the inter-station cannot be covered within the target time $to_{k_{0i}}$. In this case, when remotoring velocity has reached its lower value, the coasting velocity will be modified in the same velocity increments Δv until the restriction (31) of minimum difference between coasting and remotoring velocity $vdiff_{min}$ is met.

$$vr_{min} < v_r' \tag{30}$$
$$vdiff_{min} < v_d' - v_r' \tag{31}$$

2. If the train is coasting (it is approaching the remotoring point), the remotoring velocity v_r is reduced until the minimum remotoring velocity restriction is met. If this is not sufficient to achieve the target time $to_{k_{0i}}$, the coasting velocity vd is then reduced until the minimum difference between coasting and remotoring velocity $vdiff_{min}$ restriction is met or until the target time is reached.

It is worth noting that, in the case when the driving command is speed regulation v_{reg} (to maintain a constant velocity), the procedure of the model is similar: the regulation velocity v_{reg}' is reduced in velocity increments Δv until the target time to_n is achieved or until the minimum regulation velocity restriction $v_{reg.min}$ is reached

$$v_{reg.min} < v_{reg}' \tag{32}$$

IV. SIMULATOR OF THE MASS TRANSIT LINE

To evaluate the benefits of the proposed algorithm, a simulator based on a real mass transit line has been designed with the ability to model the movement of N trains simultaneously. This simulator (see Fig. 2) consists, on one hand, of an onboard control that includes the ATO, which receives the driving commands generated by the predictive algorithm equipped with CBTC technology and delivers to the train the force that the motor must exert. The onboard control will read the position, time, and speed of each train, and those data will be used as inputs to repeat the process described in Fig. 2.

All trains within the convoy are considered identical and are modeled in the same way. For each train, its length l, mass m, and three coefficients a_{res}, b_{res}, and c_{res} involved in rolling resistance are defined [49]. Therefore, the running resistance force F_{res} is defined as

$$F_{res} = a_{res} + b_{res}v + c_{res}v^2 \tag{33}$$

The track grade is defined as gr being positive if it is increasing and negative if it is decreasing. Considering the resistance force due to the track slope F_{gr}, it is obtained

$$F_{gr} = m \cdot g \cdot \text{gr} \tag{34}$$

The motor force F_m that the train needs to apply is obtained from the implemented ATO algorithm, where a distinction is made between acceleration and braking situations. The parameter k is the gain of the proportional controller, and the variable a_0 is the ratio of traction force which is saturated between 0 (coasting) and 1 (maximum traction effort).

In the case of acceleration, considering the maximum track velocity v_{max} and the maximum traction force dependent on the train velocity $F_{max}(v)$, the calculation is performed as follows:

$$a_0 = k(v_{max} - v) \tag{35}$$
$$F_m = a_o F_{max}(v) \tag{36}$$

The model takes into account the driving commands received. When the train reaches the current v_d command it starts coasting (null traction effort F_m). When the train reaches the current v_r command the traction effort is calculated again as (36) to accelerate.

In the case of braking, three scenarios are considered. The first occurs when braking is necessary due to a reduction in the maximum track velocity. The second scenario happens when the train is approaching a station, and the third scenario is executed when train $i+1$ detects an excessive approach to train i, typically due to situations like excessive delays

or unplanned stops along the route. For each of the three previous scenarios, a braking curve is calculated so that the train can observe these limitations.

In this case, defining the ATO parameters k_{br}, deceleration decel, and the velocity limit for the train v_{ns} calculated as the minimum speed at the train's position of the braking curves, determined by the most restrictive braking curve resulting from the three situations, the calculation is as follows:

$$a_0 = k_{br}\,(v_{ns} - v_i) - \text{decel} + \text{gr}{\cdot}g \tag{37}$$

$$F_m = a_0 \text{mi} \tag{38}$$

where mi is the total inertial mass of the train including the rotatory inertia mass.

It is important to mention that, when calculating the traction effort for both acceleration and braking, the variations are such that a jerk limit of 0.7 m/s^3 is not exceeded to ensure passenger comfort.

Given the forces F_{res}, F_{gr} and F_m calculated in equations (33), (34), and (36) or (38), the acceleration ac of the train is calculated at each simulation step st, defined by the time increment Δt:

$$\text{ac(st)} = \frac{F_m - F_{res} - F_{gr}}{\text{mi}} \tag{39}$$

And, in turn, the values of velocity v and the train's position pos are deduced from the acceleration at each simulation step

$$v\,(\text{st}) = v\,(\text{st}-1) + \text{ac}\,(\text{st}) \cdot \Delta t \tag{40}$$

$$\text{pos}\,(\text{st}) = \text{pos}\,(\text{st}-1) + v\,(\text{st}) \cdot \Delta t + \frac{1}{2}\text{ac}\,(\text{st}) \cdot \Delta t^2 \tag{41}$$

The multi-train simulator has been equipped with a model that quantifies delays caused by passenger boarding and alighting at stations. This phenomenon is simulated by adding an extra stop time sd_k to the nominal stop time S_{0k} and to the current dwell control action up_k, resulting in the actual stop time sr_k at station k

$$\text{sr}_k = S_{0k} + \text{up}_k + \text{sd}_k \tag{42}$$

In reference [47], it is explained that the most accurate statistical distribution to simulate these types of events is a lognormal distribution. Therefore, the model implemented in the simulator obtains the extra stop time sd_k from a lognormal distribution with a mean equal to the nominal stop time and a standard deviation of value.

V. RESULTS

The proposed traffic regulation model has been implemented and tested using the traffic simulator.

The simulator is based on a fixed-increment time advance, using a simulation step of 0.1 s. The main characteristics of the simulated loop line (travel times, stop times, ATO characteristics, track profile, speed limitations), are based on a real Spanish mass transit line. The implemented system consists of 35 stations and 15 trains, and the parameters characterizing the line have been defined with a nominal stop time of 20 s per station and a nominal interval of 210 s. The nominal travel time between stations depends on the distances between them and the track layout, varying between 49 s for the shortest interstation and 116 s for the longest interstation.

Additionally, the line configuration does not allow to recover delays during station stops, but the dwell time can be extended up to a maximum of 20 s beyond the nominal stop time. Similarly, the running time that a train can lose or gain at each interstation respect to the nominal one is defined by the range of speed profiles available to be executed at each interstation.

The CBTC control cycle has been adjusted to 1 s, so control actions are computed and sent at this rate, regardless of whether the train is stopped at a station or in transit.

A. SCENARIOS CONSIDERED

In Scenario 1, the ATO Driving Command generator, described in Section III-B, is tested by requesting a new running time at intermediate points between two consecutive stations, obtaining the new speed profile that the train must follow to comply with the target arrival time.

In Scenario 2 the evolution of the traffic is studied when a delay of 120 seconds arises to one train in the convoy. In this case, no uncertainty is applied to the stop times due to passenger boarding and alighting, as the goal is to study the recovery transient of the traffic regulation algorithm.

Finally, the traffic evolution is examined under normal operating conditions when dwell times depend on statistical probabilities resulting from disturbances caused by passengers (Scenario 3).

The selection of the weights in the cost function (equation (25)) has been chosen as follows. The weights of the regularity of interval and the stop and travel control actions have been defined equally to promote the interval objective ($q = a = b = 1$). On the other hand, the schedule weight has been set to $p = 0.15$ to achieve total recovery of delays once the trains' intervals have been regulated. The weight of the slack variable is set to a big value to be used only when necessary ($c = 1.000$). Finally, the simulation horizon in Scenario 2 and 3 has been defined as one complete round on the metro line ($L = 35$ stations), big enough to predict completely the recovery of delays of Scenario 2.

B. TESTING PHILOSOPHY

The performance of three different controllers that correspond to different controllers is compared to demonstrate the advantages of the predictive traffic regulation algorithm proposed equipped with continuous communication and a high bandwidth (which permits to use the generated Pareto curve explained in Section III-B):

- Controller (A) implements the proposed mathematical predictive model, explained in Section III, to generate the control actions in a line equipped with a discrete control center to train communication system, with low bandwidth, offering a choice of four predesigned speed

profiles. Delay quantification and control action generation are only performed at stations.

- Controller (B) implements the proposed mathematical predictive model, explained in Section III, to generate the control actions in a line equipped with a discrete control center to train communication system, with high bandwidth, offering all the velocity profiles existent in the Pareto curve. Delay quantification and control action generation are only performed at stations.
- Controller (C) implements the proposed mathematical predictive model, explained in Section III, to generate the control actions in a line equipped with a continuous radio communication signalling system with high bandwidth, offering all the velocity profiles existent in the Pareto curve. This last controller constitutes the regulator where the proposed predictive algorithm equipped with CBTC is implemented. Delay quantification and control action generation are continuously performed.

The performance indicators for the proposed traffic regulator will be determined by the objectives in the cost function: deviations from the nominal schedule, deviations from the nominal interval, and the evolution of control actions throughout the simulation scenario.

C. COMPUTATIONAL PERFORMANCE

The predictive optimization mathematical model generating control actions has been implemented using the MATLAB programming language. The lsqlin solver is employed, which can solve linear least squares problems with linear constraints.

The problems have been solved using an Intel Core i7 processor with a base frequency of 2.6 GHz. The average time elapsed in generating control actions is 0.85 seconds. This time is sufficiently fast to be applied to a control cycle of 1 second, which is the frequency at which CBTC technology recalculates train velocity profiles based on the provided control actions.

D. SIMULATIONS RESULTS

1) SCENARIO 1. SIMULATION OF THE ATO DRIVING COMMAND GENERATOR IN ONE INTERSTATION

The first scenario described in Section V-A is presented in this section. The selected interstation has a nominal running time of 49.5 seconds, designed according to a coasting velocity of 45 km/h and a remotoring velocity of 30 km/h. Due to a traffic disturbance, it is supposed a control command of 4 seconds slower than the nominal interstation run time.

Two scenarios are presented to demonstrate the operation of the calculator of the ATO driving commands: in the first situation, Scenario 1.1, the speed profile recalculation command is received at the beginning of the run while the train is accelerating; in the second situation, Scenario 1.2, the speed profile recalculation command is received while the train is coasting, after having reached the coasting velocity.

TABLE 2. Scenario 2 results.

	CONTROLLER A	CONTROLLER B	CONTROLLER C
SchD [s^2]	262292.76	292970.59	314633.52
HD [s^2]	149898.56	136596.20	121392.35
RCA [s^2]	12858.22	4063.24	3599.34
SCA [s^2]	4963.46	1895.62	1371.30
SG [s^2]	5.59	1.50	0.70
J [s^2]	212586.61	188546.27	174999.32
E [kWh]	38323.38	35939.76	35915.59

The objective of the CBTC speed profile calculator is to find new ATO driving commands that allow extending the interstation travel time by 4 seconds. In Fig. 7, the speed profile obtained in the two scenarios are shown.

It is observed that, depending on the situation, different strategies are employed to achieve the new target time. In Scenario 1.1, both coasting and remotoring velocities have been adjusted to reach the goal because the train has not started to coast when calculating the new speed profile. In the second Scenario 1.2, only the remotoring velocity has been modified given that the train is coasting when the new speed profile is generated. The obtained speed profiles performed the target running time 53.5 s.

2) SCENARIO 2. SIMULATION OF THE TRAFFIC REGULATION ALGORITHM IN A COMPLETE LINE WHEN ONE TRAIN IS INITIALLY DELAYED

A delay of 120 seconds is applied to one train of the convoy, and the goal is to analyze the system's behavior during the transient period until the nominal schedule is recovered. To analyze this, the metrics used are the terms of the cost function (J), namely, the deviation from the nominal schedule (SchD), the deviation from the nominal interval (HD), the control actions for travel (RCA) and stop (SCA) executed and the slack variable (SG), with all previous terms squared and summed for all trains and all stations.

Additionally, the energy consumption (E) of the convoy has been calculated to compare the three traffic regulators in terms of both operation and energy consumption.

In Table 2, the results for the previously mentioned parameters and the energy consumption for the three controllers are presented, and in Table 3, the percentage improvements of the CBTC-equipped regulator (Controller C) over the other two controllers are shown.

The proposed traffic regulator of CBTC lines represents a significant improvement over the other two regulators in all parameters except for the deviation from the nominal schedule. To enhance the regularity of the nominal headway between trains, it is necessary to compromise schedule adherence. The balance between headway and timetable adherence is represented by the cost function (J), which is improved by the proposed controller by 17.68% and 7.18% compared to Controller A and B respectively.

TABLE 3. Scenario 2 percentual results of Controller C.

	VS CONTROLLER A	VS CONTROLLER B
SchD [s^2]	-19.96%	-7.39%
HD [s^2]	19.02%	11.13%
RCA [s^2]	72.01%	11.42%
SCA [s^2]	72.37%	27.66%
SG [s^2]	87.48%	53.33%
J [s^2]	17.68%	7.18%
E [kWh]	6.28%	0.07%

In terms of energy consumption, in the face of significant delays in operation, the proposed regulator in this article is capable of consuming 6.28% less energy than traditional regulators based on discrete communications (Controller A) thanks to the high resolution of driving commands. It can be observed that controllers B and C present similar energy consumption results. That means that, although continuous communication improves headway regularity, the effect on energy consumption can be neglected.

To better understand the results, Fig. 8 and Fig. 9 illustrate the evolution of the delay recovery transient period. Fig. 8 shows the delay evolution of the initially delayed train and of the preceding train $(i-1)$ with the 3 controllers described. Fig. 9 shows the delay evolution of the initially delayed train and of the following train $(i+1)$ with the 3 controllers.

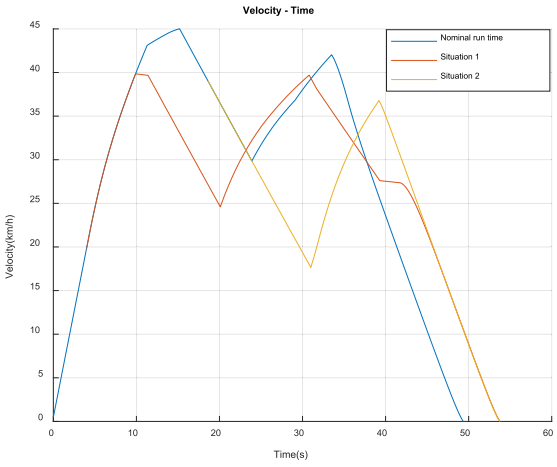

FIGURE 7. ATO driving commands recalculation.

These two trains have been chosen for representation as they are the ones most affected by the delay-induced velocity regulation.

The initially delayed train recovers the schedule running as fast as possible, taking into account that the time that can be recovered is different at each interstation. The transient of the preceding train starts running slower than the nominal time to reduce the headway deviation with the delayed train. Once this headway deviation is small enough, the preceding train starts to run faster to recover its own delay. As can be seen in Fig. 8, the advantage of continuous communication is that

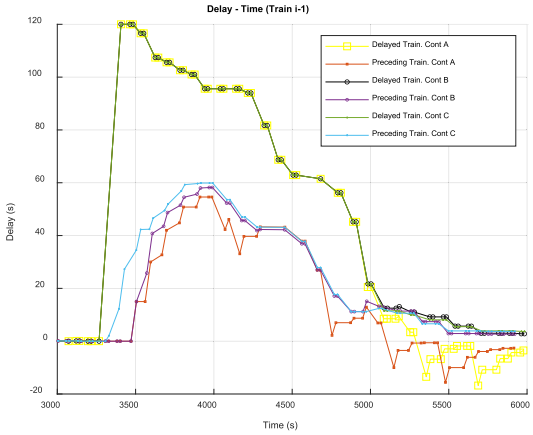

FIGURE 8. Transient evolution $(i-1)$.

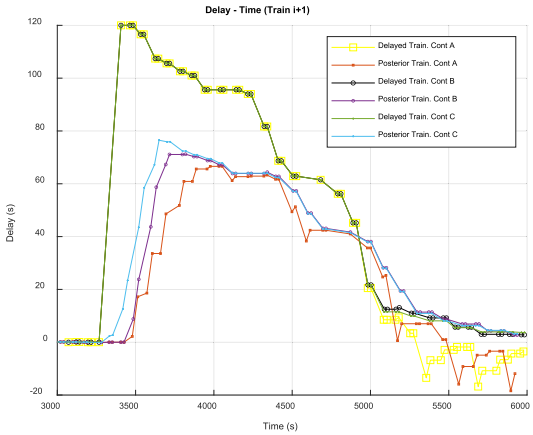

FIGURE 9. Transient evolution $(i+1)$.

the preceding train reacts earlier when the train is running. Similarly, the follower train initially increases its own delay to separate from the delay train, and runs faster when the headway delay is reduced (Fig. 9). As in the previous case, Controller C allows an earlier reaction.

Fig. 10, Fig. 11, and Fig. 12 depict the evolution of the deviation from the nominal headway for the preceding and follower train. As can be seen in these figures, using Controller C, the early reaction of the preceding train causes its headway delay rises some stations before the other controllers. However, it allows it to get closer to the delayed train to reduce its headway deviation. On the other hand, the early reaction of the follower train allows him to maintain more distance with the delayed one and, as a consequence, experiments significantly lower headway deviation.

To conclude the results of scenario 2, Fig. 14 and Fig. 15 show the evolution of the convoy's sum of squared deviation from the schedule and the evolution of the convoy's sum of squared deviation from the headway over time, respectively.

Once again, the improvement in maintaining the nominal interval can be observed due to the proposed regulator, even though there is a sacrifice in adhering to the nominal schedule according to the preferences defined in the objective function weights.

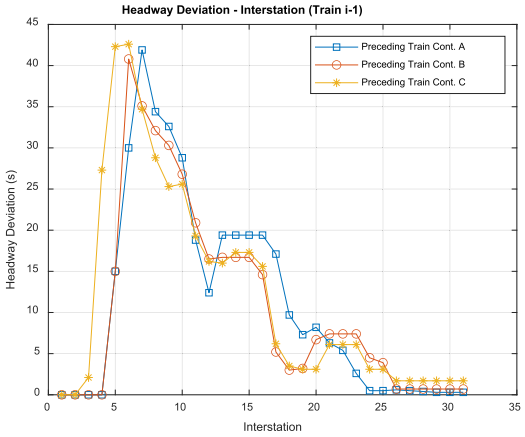

FIGURE 10. Headway deviation of the preceding train ($i-1$).

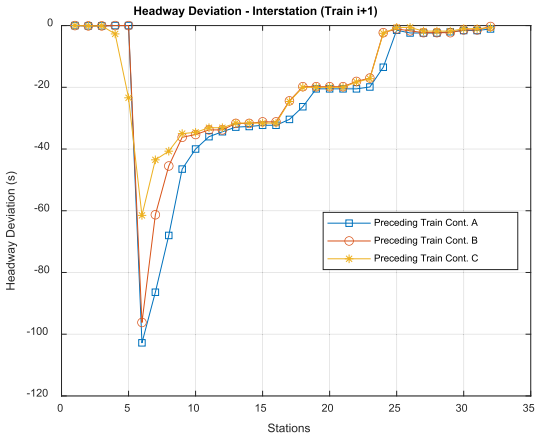

FIGURE 11. Headway deviation of the follower train ($i+1$).

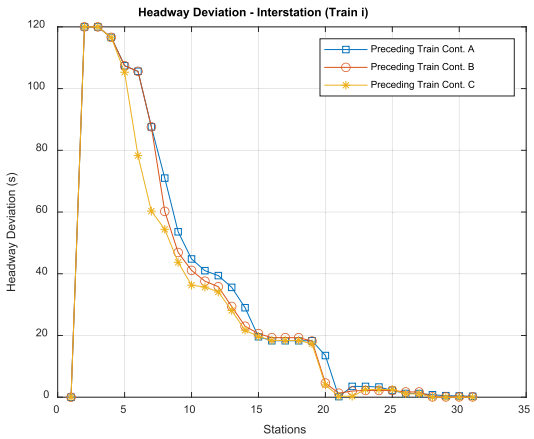

FIGURE 12. Headway deviation of the delayed train.

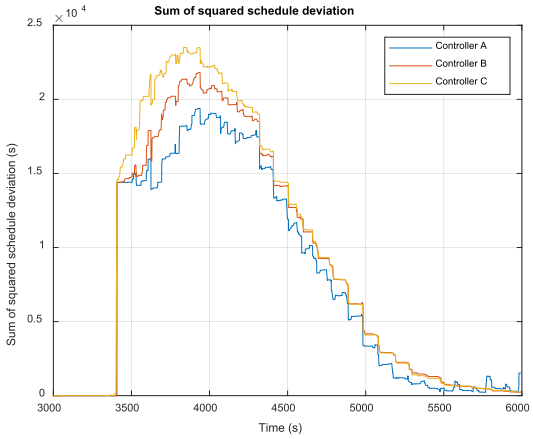

FIGURE 13. Sum of squared schedule deviation. Scenario 2.

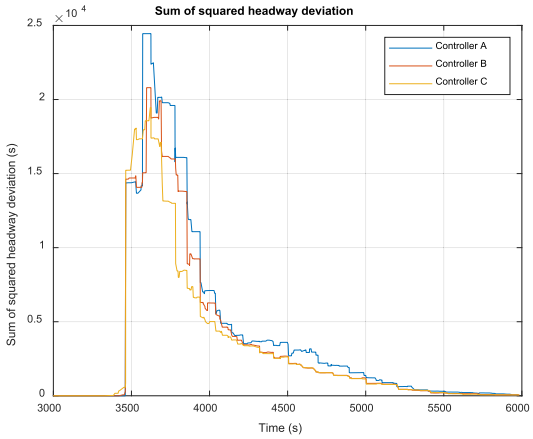

FIGURE 14. Sum of squared headway deviation. Scenario 2.

TABLE 4. Scenario 3 results.

	CONTROLLER A	CONTROLLER B	CONTROLLER C
SchD [s^2]	24498.45	18258.59	16360.36
HD [s^2]	22123.07	11654.82	11328.14
RCA [s^2]	9068.27	4117.42	4069.80
SCA [s^2]	587.62	4.95	4.71
SG [s^2]	38060.42	24134.13	22138.80
J [s^2]	26585.54	25174.50	25145.06
E [kWh]	24498.45	18258.59	16360.36

3) SCENARIO 3. SIMULATION OF THE TRAFFIC REGULATION ALGORITHM IN A COMPLETE LINE WITH RANDOM DELAYS AT EACH STATION

Finally, Scenario 3 is introduced, where the aim is to analyze the system's behavior under nominal operating conditions considering the statistical dwell time deviations. In this scenario, no initial delays are imposed on the trains (as in Scenario 2). Instead, the system evolves by introducing noisy dwell times at the stations due to passenger boarding and alighting. This phenomenon has been simulated using a log-normal distribution with a mean of the nominal station stop time (20 seconds) and a standard deviation of 5 seconds [47]. Specifically, in this scenario, the delays occurring at the stations are relatively small, not exceeding 24 seconds in the most unfavorable case. The simulation window is long enough to observe the effects of the three regulators over time.

Like Scenario 2, Table 4 displays the results of the components of the objective function and the energy consumption for the three regulators. Additionally, Table 5 presents the percentage improvements of the CBTC-equipped (Controller C) over the other two controllers.

TABLE 5. Scenario 3 percentual results of Controller C.

	VS CONTROLLER A	VS CONTROLLER B
SchD [s^2]	33.22%	10.40%
HD [s^2]	48.79%	2.80%
RCA [s^2]	55.12%	1.16%
SCA [s^2]	99.20%	4.85%
SG [s^2]	41.83%	8.27%
J [s^2]	5.42%	0.12%
E [kWh]	33.22%	10.40%

In this scenario that represents the normal traffic of the line with small disturbances at each train departure, the proposed Controller C significantly improves all the studied parameters. Based on the results, both the deviation from the nominal schedule and the deviation from the nominal headway are improved.

Additionally, comparing Controller C with Controller A, run control actions are reduced by half, and stop control actions are nearly eliminated (a reduction of 99.20%). Passenger comfort at stations is therefore increased by Controller C, because dwell time increase is unpleasantly perceived by passengers. Comparing Controller C with Controller B, run control actions are reduced 1.16%, and stop control actions are reduced 4.85%.

Finally, in terms of energy efficiency, implementing the proposed Controller C would result in an energy savings of 5.42% compared to what would be consumed with the low-bandwidth Controller A.

VI. CONCLUSION

Traffic regulation systems are crucial in mass transit lines to prevent line instability and improve the quality of service, dealing with the frequent delays of this kind of line.

The traffic regulation system constantly supervises the traffic performance in terms of timetable and headway adherence, and regulates the dwell time and the running time of trains.

The present paper proposes a new centralized predictive traffic regulation model for a railway mass transit line equipped with CBTC signalling system. This model takes advantage of continuous communications between the centralized control center and trains, to send control actions at any time and at any point of the line.

The contributions of this algorithm include a continuous measure of schedule and headway deviations. Based on that information, the proposed mathematical predictive control algorithm calculates the running time and stop control actions using a quadratic programming optimization model that includes the traffic constraints. The main objective of the control is the minimization of the timetable and the headway deviations weighted according to operators' preferences. Then, the proposed generator of updated ATO driving commands modifies the speed profile of the trains when a new target running time is provided by the predictive control for trains running between stations, permitting the early correction of delays.

To verify the impact of the proposed model on the operation of a mass transit line, this algorithm has been implemented and tested by means of a detailed simulation model of a real Spanish metro line. Two traffic cases have been analyzed.

The traffic case considering a significant single delay in a train is used to study the system's transient response of the proposed CBTC regulation model compared to traditional regulation models based on discrete control center to train communications. According to the results, it can be concluded that when a train experiences a significant delay, the proposed model improves the adherence to nominal headway by 19%, at the expense of deviating from the nominal schedule by a similar proportion. In this case, travel and stop control actions are reduced to about one-fourth of the control actions generated with traditional regulation systems, which implies a passenger comfort increase. Globally, the cost function that reflects the timetable and headway preferences is improved by 18%. In addition, energy consumption is reduced by 6.3%.

The traffic case under normal operating conditions considers random delays at each station. In this case, the adherence to the schedule and nominal headway improves by 33% and 49% respectively, due to the capability to provide an early reaction to the delays that arise in the line. Furthermore, control actions are significantly reduced, resulting in better passenger comfort, and the energy consumption is reduced by 5.4%.

These results show that modern signalling systems based on continuous communications, that permit a better transport capacity, require the design and implementation of new regulation models to improve traffic regularity, energy consumption, and quality of service.

REFERENCES

[1] V. R. Vuchic, *Urban Transit Systems and Technology*. Hoboken, NJ, USA: Wiley, 2007.

[2] D. Emery, "Towards automatic train operation for long distance services: State-of–the art and challenges," in *Proc. 17th Swiss Transp. Res. Conf. Ascona Switz.*, May 2017, pp. 1–13.

[3] M. Domínguez, A. Fernández, A. P. Cucala, and P. Lukaszewicz, "Optimal design of metro automatic train operation speed profiles for reducing energy consumption," *Proc. Inst. Mech. Eng., F, J. Rail Rapid Transit*, vol. 225, no. 5, pp. 463–474, Sep. 2011, doi: 10.1177/09544097jrrt420.

[4] C. S. Chang and S. S. Sim, "Optimising train movements through coast control using genetic algorithms," *IEE Proc. Electr. Power Appl.*, vol. 144, no. 1, p. 65, 1997, doi: 10.1049/ip-epa:19970797.

[5] A. Fernández-Rodríguez, A. P. Cucala, and A. Fernández-Cardador, "An eco-driving algorithm for interoperable automatic train operation," *Appl. Sci.*, vol. 10, no. 21, p. 7705, Oct. 2020, doi: 10.3390/app10217705.

[6] A. González-Gil, R. Palacin, P. Batty, and J. P. Powell, "A systems approach to reduce urban rail energy consumption," *Energy Convers. Manage.*, vol. 80, pp. 509–524, Apr. 2014, doi: 10.1016/j.enconman.2014.01.060.

[7] V. Van Breusegem, G. Campion, and G. Bastin, "Traffic modeling and state feedback control for metro lines," *IEEE Trans. Autom. Control*, vol. 36, no. 7, pp. 770–784, Jul. 1991, doi: 10.1109/9.85057.

[8] P. Kecman, F. Corman, A. D'Ariano, and R. M. P. Goverde, "Rescheduling models for railway traffic management in large-scale networks," *Public Transp.*, vol. 5, nos. 1–2, pp. 95–123, Sep. 2013, doi: 10.1007/s12469-013-0063-y.
[9] J. Yin, X. Ren, S. Su, F. Yan, and T. Tao, "Resilience-oriented train rescheduling optimization in railway networks: A mixed integer programming approach," *IEEE Trans. Intell. Transp. Syst.*, vol. 24, no. 5, pp. 4948–4961, May 2023, doi: 10.1109/TITS.2023.3236004.
[10] Y. Zhu and R. M. P. Goverde, "Dynamic railway timetable rescheduling for multiple connected disruptions," *Transp. Res. C, Emerg. Technol.*, vol. 125, Apr. 2021, Art. no. 103080, doi: 10.1016/j.trc.2021.103080.
[11] B. Sharma, P. Pellegrini, J. Rodriguez, and N. Chaudhary, "A review of passenger-oriented railway rescheduling approaches," *Eur. Transp. Res. Rev.*, vol. 15, no. 1, p. 14, May 2023, doi: 10.1186/s12544-023-00587-0.
[12] C. Zhang, Y. Gao, V. Cacchiani, L. Yang, and Z. Gao, "Train rescheduling for large-scale disruptions in a large-scale railway network," *Transp. Res. B, Methodol.*, vol. 174, Aug. 2023, Art. no. 102786, doi: 10.1016/j.trb.2023.102786.
[13] F. Corman, A. D'Ariano, A. D. Marra, D. Pacciarelli, and M. Samà, "Integrating train scheduling and delay management in real-time railway traffic control," *Transp. Res. E, Logistics Transp. Rev.*, vol. 105, pp. 213–239, Sep. 2017, doi: 10.1016/j.tre.2016.04.007.
[14] S. Araya and S. Sone, "Traffic dynamics of automated transit systems with pre-established schedules," *IEEE Trans. Syst. Man, Cybern.*, vol. SMC-14, no. 4, pp. 677–687, Jul. 1984, doi: 10.1109/TSMC.1984.6313344.
[15] X. Cai and C. J. Goh, "A fast heuristic for the train scheduling problem," *Comput. Oper. Res.*, vol. 21, no. 5, pp. 499–510, May 1994, doi: 10.1016/0305-0548(94)90099-x.
[16] A. Higgins, E. Kozan, and L. Ferreira, "Heuristic techniques for single line train scheduling," *J. Heuristics*, vol. 3, no. 1, pp. 43–62, Mar. 1997, doi: 10.1023/a:1009672832658.
[17] C. S. Chang and B. S. Thia, "Online rescheduling of mass rapid transit systems: Fuzzy expert system approach," *IEE Proc. Electr. Power Appl.*, vol. 143, no. 4, p. 307, Jul. 1996, doi: 10.1049/ip-epa:19960311.
[18] S.-C. Chang and Y.-C. Chung, "From timetabling to train regulation—A new train operation model," *Inf. Softw. Technol.*, vol. 47, no. 9, pp. 575–585, Jun. 2005, doi: 10.1016/j.infsof.2004.10.008.
[19] M. Zhou, Z. Hou, X. Wu, H. Dong, and F.-Y. Wang, "Integration of train regulation and speed profile optimization based on feature learning and hybrid search algorithm," *IEEE Trans. Computat. Social Syst.*, vol. 11, no. 2, pp. 2535–2544, Apr. 2024, doi: 10.1109/tcss.2023.3303473.
[20] S. Li, L. Yang, Z. Gao, and K. Li, "Robust train regulation for metro lines with stochastic passenger arrival flow," *Inf. Sci.*, vol. 373, pp. 287–307, Dec. 2016, doi: 10.1016/j.ins.2016.09.019.
[21] X. Xu, K. Li, and X. Li, "A multi-objective subway timetable optimization approach with minimum passenger time and energy consumption," *J. Adv. Transp.*, vol. 50, no. 1, pp. 69–95, Jan. 2016, doi: 10.1002/atr.1317.
[22] J.-W. Sheu and W.-S. Lin, "Energy-saving automatic train regulation using dual heuristic programming," *IEEE Trans. Veh. Technol.*, vol. 61, no. 4, pp. 1503–1514, May 2012, doi: 10.1109/TVT.2012.2187225.
[23] D. Kraay, "Learning methods in optimisation: With applications to railroad control," Wharton School, Decisions Sci. Dept., Univ. Pennsylvania, Philadelphia, PA, USA, 1993.
[24] W.-S. Lin and J.-W. Sheu, "Optimization of train regulation and energy usage of metro lines using an adaptive-optimal-control algorithm," *IEEE Trans. Autom. Sci. Eng.*, vol. 8, no. 4, pp. 855–864, Oct. 2011, doi: 10.1109/TASE.2011.2160537.
[25] C. E. García, D. M. Prett, and M. Morari, "Model predictive control: Theory and practice—A survey," *Automatica*, vol. 25, no. 3, pp. 335–348, May 1989, doi: 10.1016/0005-1098(89)90002-2.
[26] B. Nie and Y. Tong, "A survey of applications of model predictive control to rail traffic regulation," in *Proc. China Automation Congr. (CAC)*, Nov. 2022, pp. 2461–2465, doi: 10.1109/CAC57257.2022.10054712.
[27] P. Grube and A. Cipriano, "Comparison of simple and model predictive control strategies for the holding problem in a metro train system," *IET Intell. Transp. Syst.*, vol. 4, no. 2, p. 161, Jun. 2010, doi: 10.1049/iet-its.2009.0086.
[28] G. Campion, V. Van Breusegem, P. Pinson, and G. Bastin, "Traffic regulation of an underground railway transportation system by state feedback," *Optim. Control Appl. Methods*, vol. 6, no. 4, pp. 385–402, Oct. 1985, doi: 10.1002/oca.4660060406.
[29] C. J. Goodman and S. Murata, "Metro traffic regulation from the passenger perspective," *Proc. Inst. Mech. Eng., F, J. Rail Rapid Transit*, vol. 215, no. 2, pp. 137–147, Mar. 2001, doi: 10.1243/0954409011531468.
[30] A. Fernandez, A. P. Cucala, B. Vitoriano, and F. de Cuadra, "Predictive traffic regulation for metro loop lines based on quadratic programming," *Proc. Inst. Mech. Eng., F, J. Rail Rapid Transit*, vol. 220, no. 2, pp. 79–89, Mar. 2006, doi: 10.1243/09544097f00505.
[31] S. Hao, R. Song, S. He, and Z. Lan, "Train regulation combined with passenger control model based on approximate dynamic programming," *Symmetry*, vol. 11, no. 3, p. 303, Mar. 2019, doi: 10.3390/sym11030303.
[32] H. Zhang, S. Li, and L. Yang, "Real-time optimal train regulation design for metro lines with energy-saving," *Comput. Ind. Eng.*, vol. 127, pp. 1282–1296, Jan. 2019, doi: 10.1016/j.cie.2018.02.019.
[33] S. Li, X. Zhou, L. Yang, and Z. Gao, "Automatic train regulation of complex metro networks with transfer coordination constraints: A distributed optimal control framework," *Transp. Res. B, Methodol.*, vol. 117, pp. 228–253, Nov. 2018, doi: 10.1016/j.trb.2018.09.001.
[34] S. Li, R. Liu, Z. Gao, and L. Yang, "Integrated train dwell time regulation and train speed profile generation for automatic train operations on high-density metro lines: A distributed optimal control method," *Transp. Res. B, Methodol.*, vol. 148, pp. 82–105, Jun. 2021, doi: 10.1016/j.trb.2021.04.009.
[35] A. Fernández, F. de Cuadra, and A. García, "SIRO: An optimal regulation system in an integrated control centre for metro lines," *Trans. Built Environ.*, vol. 18, pp. 299–308, Jan. 1996. [Online]. Available: https://www.witpress.com/elibrary/wit-transactions-on-the-built-environment/21/8935
[36] S. Li, B. De Schutter, L. Yang, and Z. Gao, "Robust model predictive control for train regulation in underground railway transportation," *IEEE Trans. Control Syst. Technol.*, vol. 24, no. 3, pp. 1075–1083, May 2016, doi: 10.1109/TCST.2015.2480839.
[37] B. Moaveni and S. Najafi, "Metro traffic modeling and regulation in loop lines using a robust model predictive controller to improve passenger satisfaction," *IEEE Trans. Control Syst. Technol.*, vol. 26, no. 5, pp. 1541–1551, Sep. 2018, doi: 10.1109/TCST.2017.2735945.
[38] S. Li, L. Yang, and Z. Gao, "Efficient real-time control design for automatic train regulation of metro loop lines," *IEEE Trans. Intell. Transp. Syst.*, vol. 20, no. 2, pp. 485–496, Feb. 2019, doi: 10.1109/TITS.2018.2815528.
[39] J. Luo and Y. Tong, "Constrained optimal controller design for urban metro traffic regulation," in *Proc. 40th Chin. Control Conf. (CCC)*, Jul. 2021, pp. 1657–1662, doi: 10.23919/CCC52363.2021.9550699.
[40] X. Xu and J. Xiang, "Research on train operating scheme of intercity rail transit," in *Plan, Build, and Manage Transportation Infrastructure in China*. Reston, VA, USA: ASCE, 2012, pp. 401–407, doi: 10.1061/40952(317)40.
[41] B. Jin, X. Feng, Q. Wang, and P. Sun, "Real-time train regulation method for metro lines with substation peak power reduction," *Comput. Ind. Eng.*, vol. 168, Jun. 2022, Art. no. 108113, doi: 10.1016/j.cie.2022.108113.
[42] S. Li, Y. Yuan, Z. Chen, L. Yang, and C. Yu, "Real-time train regulation in the metro system with energy storage devices: An efficient decomposition algorithm with bound contraction," *Transp. Res. Part C: Emerg. Technol.*, vol. 159, Feb. 2024, Art. no. 104493, doi: 10.1016/j.trc.2024.104493.
[43] X. Yang, B. Ning, X. Li, and T. Tang, "A two-objective timetable optimization model in subway systems," *IEEE Trans. Intell. Transp. Syst.*, vol. 15, no. 5, pp. 1913–1921, Oct. 2014, doi: 10.1109/TITS.2014.2303146.
[44] X. Wang, S. Li, S. Su, and T. Tang, "Robust fuzzy predictive control for automatic train regulation in high-frequency metro lines," *IEEE Trans. Fuzzy Syst.*, vol. 27, no. 6, pp. 1295–1308, Jun. 2019, doi: 10.1109/TFUZZ.2018.2877593.
[45] X. Wang, S. Su, Y. Cao, and X. Wang, "Robust control for dynamic train regulation in fully automatic operation system under uncertain wireless transmissions," *IEEE Trans. Intell. Transp. Syst.*, vol. 23, no. 11, pp. 20721–20734, Nov. 2022, doi: 10.1109/TITS.2022.3170950.
[46] *IEEE Standard for Communications-Based Train Control (CBTC) Performance and Functional Requirements*, Standard 14741-1999, 1999.
[47] I. Martínez, B. Vitoriano, A. Fernández, and A. Cucala, *Statistical Dwell Time Model for Metro Lines*. Billerica MA, USA: WIT Press, 2007, pp. 223–232, doi: 10.2495/UT070221.
[48] A. Fernández-Rodríguez, A. Fernández-Cardador, A. P. Cucala, M. Domínguez, and T. Gonsalves, "Design of robust and energy-efficient ATO speed profiles of metropolitan lines considering train load variations and delays," *IEEE Trans. Intell. Transp. Syst.*, vol. 16, no. 4, pp. 2061–2071, Aug. 2015, doi: 10.1109/TITS.2015.2391831.
[49] W. J. Davis, *The Tractive Resistance of Electric Locomotives and Cars*, vol. 29. Schenectady, NY, USA: General Electric, 1926.

ÁLVARO CIDONCHA received the B.S. and M.S. degrees in industrial engineering from Comillas Pontifical University, Madrid, in 2022 and 2024, respectively, where he is currently pursuing the Ph.D. degree with the Railway Research Group, Institute of Research in Technology.

His research interests include train simulation, traffic control, and railway efficient operation.

ADRIÁN FERNÁNDEZ-RODRÍGUEZ received the degree in industrial engineering from Universidad Politécnica de Madrid, in 2012, and the Ph.D. degree from Comillas Pontifical University, Madrid, in 2018.

He is currently a Research Fellow with the Railway Research Group, Institute for Research in Technology, Comillas Pontifical University. His research interests include train operation modelling, energy efficiency in railways, and nature inspired optimization.

ASUNCIÓN P. CUCALA received the degree in electrical engineering and Ph.D. degree from Comillas Pontifical University, Madrid, Spain.

She is currently the Director of the Institute for Research in Technology, a Research Fellow with the Railways Research Group, and a Full Professor with the ICAI School of Engineering, Comillas Pontifical University. Her research interests include train simulation, railways operation and control, energy efficiency in railways, and railway capacity analysis.

ANTONIO FERNÁNDEZ-CARDADOR received the degree in physics from Universidad Complutense, Madrid, Spain, and the Ph.D. degree from Comillas Pontifical University, Madrid.

He is currently a Research Fellow with the Railways Research Group, Institute for Research in Technology, and a Full Professor with the ICAI School of Engineering, Comillas Pontifical University. His research interests include train simulation, railways operation and control, eco-driving, and railway capacity.